

Island and lake size distributions in Gradient Percolation

S. S. Manna

*Satyendra Nath Bose National Centre for Basic Sciences,
Block-JD, Sector-III, Salt Lake, Kolkata-700106, India*

The well known problem of gradient percolation has been revisited to study the probability distribution of island sizes. It is observed that like the ordinary percolation, this distribution is also described by a power law decaying function but the associated critical exponents are found to be different. Because of the underlying gradient for the occupation probability, the average value of the island sizes also has a gradient. The variation of the average island size with the probability of occupation along the gradient has been studied together with its scaling analysis. Further, we have introduced and studied the gradient bond percolation and on studying the island size distribution statistics, we have obtained very similar results. We have also studied the characteristics of the diffusion profile of the particle system on a lattice which is initially half filled and half empty. Here also we observe the same value for the island size probability distribution exponent. Finally, the same study has been repeated for the nonlinear gradient percolation and the value of the island size distribution exponent is found to be a function of the strength of the nonlinear parameter.

PACS numbers:

I. INTRODUCTION

When the atoms of a solid material of type A diffuses into another solid material of type B, and vice versa, the properties of the mixing region have been found to be very interesting. For example, when the junction of two conducting materials are heated to make the electrical contact the diffusion of both types of conducting atoms takes place.

During early 1980s the statistical properties of the mixing region had attracted a lot of research interests [1]. In particular, studying the structure and properties of the interface of either type of solids had received much attention. There were many reasons for that. For example, it had been found that the interface has a fractal structure up to the diffusion length scale [2, 3]. Secondly, the interface sites have a Gaussian density profile. The dispersion of the Gaussian profile grows with time [1].

Models of the diffusion processes of one species of atoms into another species of atoms gave rise to the concept of gradient percolation [1–3]. Here the density gradients of A atoms (and B atoms) have been created along the $+x$ (and $-x$) axis only. Let the density profile of A atoms be denoted by $p(x, t)$ depending on both the space (x) as well as the time (t) coordinates. It had been shown that the density profile follows a decaying complementary error function: $p(x, t) = \text{erfc}(x/\ell_D)$, where $\ell_D = 2(Dt)^{1/2}$ is the time dependent diffusion length [8]. One side of the lattice has been enriched with A atoms, whereas its opposite side has the high density of B atoms and the intermediate region has the mixture of A and B atoms. However, in the simulation process the actual diffusion of atoms have not been executed. Instead, the independent positional configurations of A and B atoms have been generated using the density variable $p(x, t)$ as the probability of occupation of A atoms similar to the percolation problem.

The problem of Percolation is considered as one of

the simplest but non-trivial models of statistical physics. This model is typically defined on a regular lattice as a binary state problem. Every lattice site is randomly occupied with a tunable probability p and left vacant with probability $(1 - p)$. This process thus mimics the order-disorder transition taking place at a critical value of p_c [4–7]. It has been shown that the fractal dimension D_h of the ‘hull’ or outer boundary of percolation clusters close to criticality is 1.74 ± 0.02 [9].

The model of linear gradient percolation has been defined on a two dimensional substrate, e.g., a square lattice of finite size [2, 3]. It was found that instead of the actual density profile of the diffusing A atoms, a simple time independent linear profile $p(x)$ for the probability of occupation with constant gradient keeps all static properties intact. Very interestingly, it has been found that the occupation probability corresponding to the mean x position of the A atoms on the interface is the ordinary site percolation threshold p_c of the same lattice. This information had helped in estimating the value of p_c more accurately. A perimeter generating random walk had been devised to trace all A atoms on the interface [10]. Using this method the percolation threshold of the square lattice had been estimated very accurately which is $p_c = 0.59275 \pm 0.00003$ [11, 12]. Further, the fractal dimension d_f of the interface has been estimated to be exactly equal to $7/4$ which is the fractal dimension of the perimeter of the spanning clusters at the percolation thresholds of the ordinary percolation. Gradient percolation is still an active area of research [13].

Following the terminologies used in [2] we assume that an arbitrary random configuration of A and B atoms of gradient percolation has both “infinite A” cluster and “infinite B” cluster on two opposite sides of the lattice. In addition, at the middle region of the lattice there are many small finite size clusters of both types of atoms, which are called the “islands” of A atoms within the sea of B atoms and the “lakes” of B atoms within the sea of

A atoms.

Question is, what may be the probability distributions of the sizes of these islands and lakes? To the best of our knowledge this issue had not been explored in the literature till date. Therefore, we numerically study these distributions from different approaches and report the results in this paper.

In the next section II we describe our simulations and results of gradient site percolation on the square lattice. Here we have studied the probability distribution of island sizes and their scaling analysis. Further, we have studied the variation of the average values of the island sizes along the direction of the probability gradient. In section III we have introduced the gradient bond percolation model and have studied the same quantities associated with island sizes in this model as well. Later, in section IV we have studied the relaxation of an initially dense system of particles using the random walk diffusion dynamics. Primarily, we have focused to the probability distribution of the island sizes and observed that the associated exponent is different from that of the ordinary percolation in two dimension. Finally, the non-linear gradient percolation has been studied in section V with tunable strength parameter. We summarize in section VI.

II. ISLANDS IN GRADIENT SITE PERCOLATION

We first identify the finite size islands. On a square lattice of size $L \times L$, periodic along the y axis, we fill up the lattice randomly using a probability function $p(x) = 1 - x/(L + 1)$ which has a linear gradient along the x -axis. All sites (x, y) on the vertical column at a fixed x have been occupied with the same probability $p(x)$. For the small values of x , the probability of occupation is high and therefore most of the sites are occupied. Fig. 1 represents a typical gradient percolation configuration where all occupied sites represent A atoms and all vacant sites represent B atoms. All the occupied sites which are connected to the left boundary at $x = 1$ constitute the infinite A cluster and are marked in blue color. As x increases, the value of $p(x)$ decreases, and small lakes of B sites appear within the infinite A cluster.

On the other hand, for $x \sim L$, the value of $p(x)$ is small, so also the sizes of the islands shown in red color. Clearly, there exists a gradient of the island sizes as well. The average size of the islands decreases as x increases. How far the infinite A cluster is extended? It can be extended deep into the infinite B cluster. However, the x coordinates of the lattice sites on the interface or on the hull of the infinite A cluster has a mean value x_c . It is now well known in the literature that the value of x_c is such that $p(x_c) = p_c$, where p_c is the percolation threshold of the ordinary site percolation on the same lattice. The interface of the infinite A cluster is defined by the sites of those A atoms which have at least one B

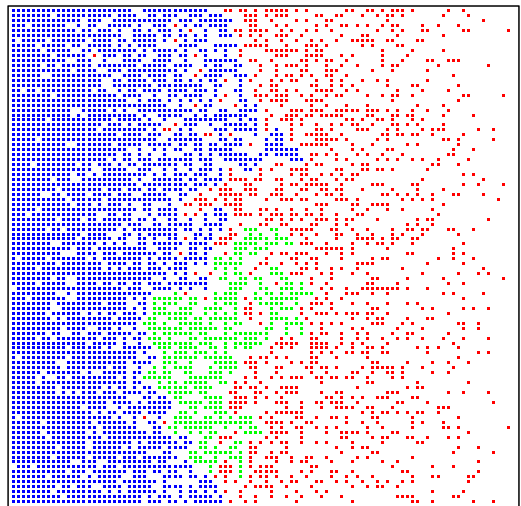


FIG. 1: On a square lattice of size $L = 100$, sites have been occupied with probability $p(x) = 1 - x/(L + 1)$ i.e., gradient $g = 1/(L + 1)$. Marked sites represent A atoms, whereas, B atoms have not been shown. The infinite A cluster has 3048 sites (blue), the largest island has 489 sites (green) and all other islands has a total of 1381 sites (red). The fraction of occupied sites is ≈ 0.4918 .

atom in the neighboring, or next neighboring site which is connected via at least one path of B atoms to the right boundary at $x = L$. Therefore, x_c is the mean of the x -coordinates of all the interface sites. Most of the finite size islands appear in the right side of the interface of infinite A cluster.

Similar to the ordinary percolation problem, we define the probability distribution $D(s, L)$ of the island sizes s of all the islands of occupied sites. Consider a typical configuration as shown in Fig. 1. We mark different islands by different label numbers (equivalent to coloring of different islands using different colors) and estimate their sizes by running a simulation process called the ‘burning algorithm’. In this process a single scan of the entire lattice enables us to identify and estimate the sizes of all distinct islands. The infinite A cluster is ignored and the frequency distribution of the sizes of the finite islands are collected in an array. This data collection process has been repeated over a large number of independent configurations and the frequencies of occurrences has been cumulatively added to the same array. Finally, this data has been normalized to obtain the probability distribution $D(s, L)$.

In Fig. 2(a), we have plotted the logarithmically binned distribution data $D(s, L)$ against s on a double logarithmic scale for three different system sizes $L = 512, 2048, 8192$ using the system size dependent linear probability gradient $g = 1/L$. All three curves exhibit the typical signatures of the power law distribution, i.e., a straight linear part in the intermediate region, followed by a sharp downward bending at some characteristic cut-

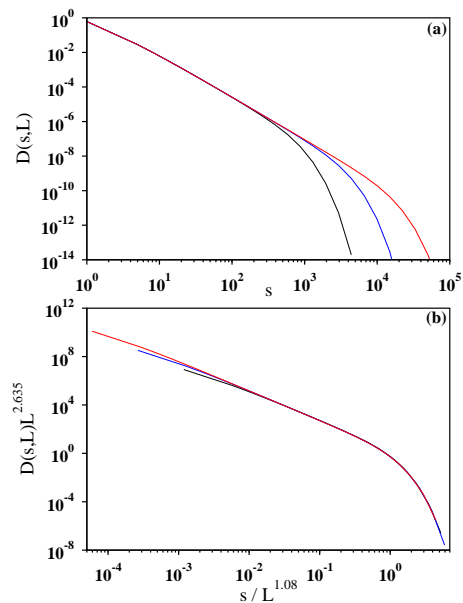


FIG. 2: (a) The probability distribution $D(s, L)$ of the island sizes have been plotted against the island size s for square lattices of size $L \times L$. The system size dependent linear probability gradient $g = 1/L$ have been used for $L = 512$ (black), 2048 (blue), and 8192 (red). (b) The same data have been replotted after scaling the x and y axes using the scale factors $L^{1.08}$ and $L^{2.635}$ respectively. The data collapse appears to be excellent implying the island size distribution exponent $\tau = 2.635/1.08 \approx 2.44$.

off island size $s_c(L) \sim L^\alpha$ which depends on the system size.

We observe that the distributions $D(s, L)$ scales nicely using suitable powers of L , like:

$$D(s, L)L^\beta \sim \mathcal{G}(s/L^\alpha) \quad (1)$$

where, $\mathcal{G}(x)$ is the scaling function such that $\mathcal{G}(x) \rightarrow x^{-\tau}$ for $x \ll 1$ and $\mathcal{G}(x) \rightarrow \text{constant}$ for $x \gg 1$. The limiting distribution $D(s) = \lim_{L \rightarrow \infty} D(s, L) \sim s^{-\tau}$ must be independent of L which leads to $\tau = \beta/\alpha$. In Fig. 2(b), a finite size scaling of the same data has been attempted. The x and y axes have been transformed by dividing the x coordinates by L^α and multiplying the y coordinates by L^β . A careful fine tuning of the values of the scaling exponents α and β yields the best collapse of the data corresponding to $\alpha \approx 1.08$ and $\beta \approx 2.635$ which gives $\tau = \beta/\alpha \approx 2.44$. It is found that the value of τ so obtained is distinctly different from the cluster size distribution exponent $\tau = 2+5/91 \approx 2.05$ of the ordinary percolation problem in two dimensions.

We have repeated the same exercise with a fixed linear probability gradient $g = 2^{-13}$ as well. On a square lattice of rectangular shape, the probability gradient is applied along the x -axis of length $L_x = 8192$ and the three different values of the width $L_y = 512, 2048,$ and 8192 have been used. In all cases the value of

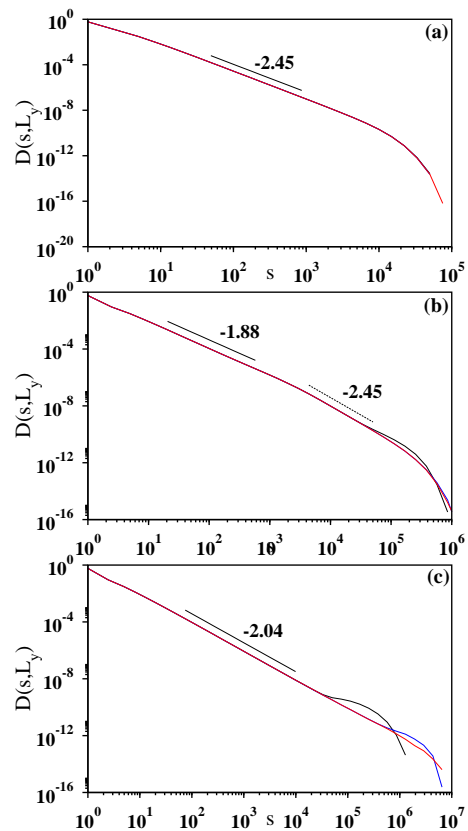


FIG. 3: Gradient percolation on the square lattice of rectangular shape having sides: $L_x = 8192$ and $L_y = 512$ (black), 2048 (blue), and 8192 (red). A fixed linear probability gradient g has been applied along the x -axis. (a) $g = 2^{-13}$: The probability distribution $D(s, L_y)$ of the island sizes have been plotted against the island size s . The value of the common slope in the intermediate region is $\tau = 2.45$. (b) $g = 2^{-17}$: It is evident that there are two regimes with different slopes. For small island sizes, the value of the slope is ≈ 1.88 (solid line), whereas, in the large island regime it is ≈ 2.45 (dashed line). (c) $g = 2^{-21}$: A major part of the intermediate region has the slope 2.04 which is close to the value of τ for ordinary percolation.

$p = p_c = 0.5927460507921$ [14] has been set exactly at $x = L_x/2$. In Fig. 3(a) we have shown the plot of the binned probability distribution data $D(s, L_y)$ against the island size s for these three system sizes. It is seen that even without any scale transformation of the coordinate axes, the data for the three system sizes collapse on top of one another. A direct measurement of the slopes of the three curves in the most linear intermediate region gives the estimate for the island size distribution exponent $\tau = 2.45 \pm 0.01$.

The same simulation has been executed using an even smaller linear probability gradient $g = 2^{-17}$ and for the same three rectangular system sizes. However, on plotting the $D(s, L_y)$ against s data in Fig. 3(b), we find that there are two regions in each curve. In the regime of small

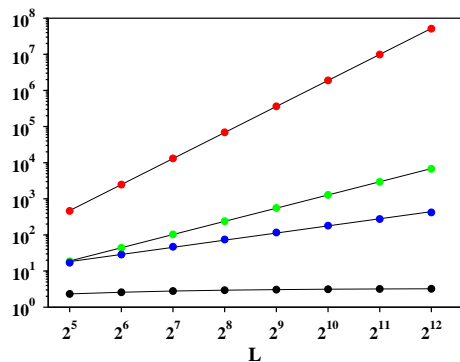


FIG. 4: The average values of the sizes of the islands (without the infinite A cluster) have been plotted here on the double logarithmic scale. The average size $\langle s(L) \rangle$ (black) of the islands, does not increase against the system size L and tends to saturate on increasing L . The other moments $\langle s^2(L) \rangle$ (blue), $\langle s_{max}(L) \rangle$ (green), and $\langle s_{max}^2(L) \rangle$ (red) vary as $L^{0.656}$, $L^{1.214}$, $L^{2.393}$ respectively.

island sizes, the slopes of the curves are quite different and nearly 1.88. On the other hand for large s regime, the slopes are the same as we obtained before, i.e., 2.45. Finally, we present the same data for $g = 2^{-21}$ in Fig. 3(c). Other than a bulge at the tail end of the distributions, the intermediate part is quite large and straight and has a common slope which is approximately 2.04, which is close to the value of the cluster size exponent 2.05 of ordinary percolation in two dimensions.

We try to explain the above three results in the following way. When we make the gradient g very small if we could have made the lattice also large, like $L_x = 1/g$ then the sample of the island sizes used for estimating the probability distribution would have picked up island of all sizes, small, medium and large. Instead, because of limitation of our computational resources, we have used a fixed value for $L_x = 8192$. Therefore, we have collected the island size data out of a box of fixed width centered around p_c . Smaller the value of the gradient g , the collected sample of island sizes is more close to p_c . This explains the crossover in the probability distribution of the island sizes where we get the single exponent $\tau \approx 2.45$ when $L_x \sim 1/g$; the value of τ being close to the ordinary percolation exponent 2.05 when $L_x \ll 1/g$ and simultaneously both values of τ for the intermediate values of g .

For the square lattices of square shapes of sizes $L \times L$, we also identify the largest island and denote its size by s_{max} . We have estimated the average value $\langle s(L) \rangle$ of the sizes of the islands and the average size $\langle s_{max}(L) \rangle$ of the largest island over all independent configurations. In Fig. 4, we have plotted $\langle s(L) \rangle$ and $\langle s^2(L) \rangle$ against the system size. On increasing L , the value of $\langle s(L) \rangle$ slightly increases initially but then tends to saturate to a constant value as L becomes large. On the other hand $\langle s^2(L) \rangle$ nicely fits to a power law growth $\langle s^2(L) \rangle \sim L^{0.656}$. Simi-

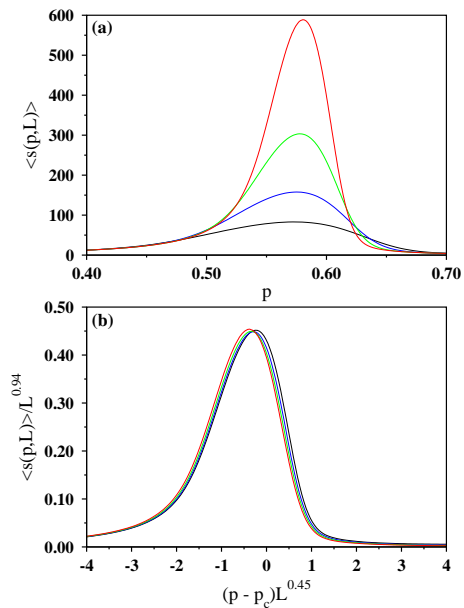


FIG. 5: (a) The average island size $\langle s(p, L) \rangle$ has been plotted against p for $L = 256$ (black), 512 (blue), 1024 (green), and 2048 (red). (b) First, the x axis has been transformed to $p \rightarrow (p - p_c)$ and then both x and y axes are scaled by the factors $L^{0.45}$ and $L^{0.94}$ respectively.

lar averages of the size of the largest cluster also fit to the power laws: $\langle s_{max}(L) \rangle \sim L^{1.214}$ and $\langle s_{max}^2(L) \rangle \sim L^{2.393}$ respectively.

Looking at the Fig. 1 it is quite clear that the island sizes also depend on the position of the island. In other words, we expect that the average island size also depends on the occupation probability gradient set in the system. Therefore, we have defined that an occupied site at x is a part of the island of size $\langle s(x, L) \rangle$ on the average. Since the probability $p(x)$ of occupation is an explicit function of x , we define the quantity $\langle s(p, L) \rangle$ instead. We have shown in Fig. 5(a) the plot of $\langle s(p, L) \rangle$ against p for the four different system sizes. Each plot has a peak which increases sharply as the system size increases. Each curve is asymmetric, i.e., on increasing p it grows slowly in comparison, but beyond the peak it falls off faster. Expectedly, the value of $p = p_{max}$ corresponding to the peak value slowly approaches to the percolation threshold p_c as the system size L increases. In Fig. 5(b) we have performed a system size dependent scaling of the same data and plotted $\langle s(p, L) \rangle / L^{0.94}$ against $(p - p_c) L^{0.45}$. The data collapse is found to be quite good.

III. ISLANDS IN GRADIENT BOND PERCOLATION

The problem of gradient percolation can also be studied in terms of lattice bonds, as in the ordinary bond

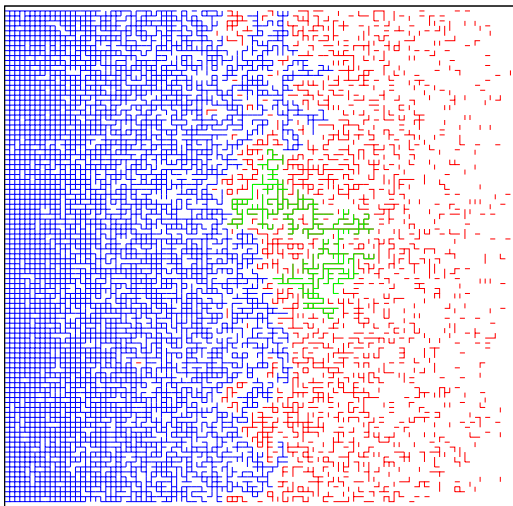


FIG. 6: On a square lattice of size $L = 100$, the upward vertical bond and the right horizontal bond from each site (x, y) have been occupied with probability $p(x) = 1 - x/L$ i.e., with gradient $g = 1/L$. The infinite A cluster has 7635 occupied bonds (blue), the largest island has 358 bonds (green) and all other islands has a total of 2339 bonds (red).

percolation model. To the best of our knowledge, the model of gradient bond percolation has not been studied yet in the literature. The percolation threshold for bond percolation has been known to be exactly $1/2$. Because of this, the set of occupied and vacant bonds are symmetric about the percolation point and we expect to get better statistics compared to the gradient site percolation.

The probability gradient $g = 1/L$ has been applied along the x -axis as before. Therefore, the position dependent bond occupation probability is $p(x) = 1 - x/L$. Here, both the upward vertical bond and the right horizontal bond from (x, y) have been occupied with probability $p(x)$. One gets a gradient bond percolation configuration when all bonds of the lattice of size $L \times L$ are either occupied with probability $p(x)$ or left vacant with probability $1 - p(x)$. For our island size calculation, the equivalent site configuration has been created by occupying the end sites of every occupied bond. As in the previous case, the burning algorithm has been applied to the resulting site configuration to estimate the island sizes, ignoring the infinite A cluster. The entire calculation has been repeated over a large number of independent configurations to obtain the probability distribution of island sizes. A typical gradient bond percolation configuration has been shown in Fig. 6.

The data for the probability distributions of gradient bond percolation have been plotted in Fig. 7(a). The above mentioned linear probability gradient have been applied to three system sizes, namely, $L = 512$, 2048, and 8192. Distributions $D(s, L)$ against s plots get separated from one another at their tail ends. However, in Fig. 7(b), an excellent data collapse of the three curves

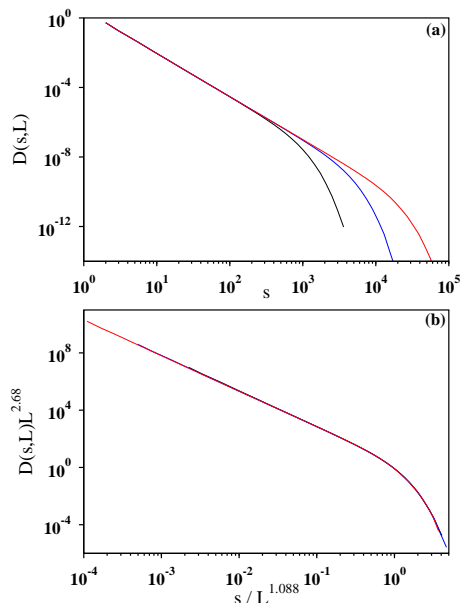


FIG. 7: For the gradient bond percolation: (a) The probability distribution $D(s, L)$ of the island sizes have been plotted against the island size s for square lattices of size $L \times L$. The system size dependent linear probability gradient $g = 1/L$ have been used for $L = 512$ (black), 2048 (green), and 8192 (red). (b) The same data have been replotted after scaling the x and y axes using the scale factors $L^{1.088}$ and $L^{2.68}$ respectively. The data collapse appears to be excellent implying the island size distribution exponent $\tau = 2.68/1.088 \approx 2.46$.

were possible by scaling the axes using factors which are different powers of L . The best values of the scaling exponents have been estimated to be 1.088 and 2.68 for the x and y axes respectively, giving the value of the exponent $\tau = 2.68/1.088 \approx 2.46$.

The same probability distribution has been studied for a rectangular system of sizes $L_x = 8192$ and $L_y = 512$, 2048, and 8192 with fixed gradients $g = 2^{-13}$, 2^{-17} , and 2^{-21} . A similar crossover between τ values 2.45 and 2.05 as reported in 3 has been observed for the gradient bond percolation as well. Further, very similar results for the variation of the average values of the island sizes as reported in 4 and 5 have been obtained. We therefore chose not to exhibit the similar plots here.

IV. ISLANDS NEAR THE INTERFACE OF DIFFUSION FRONT

We have also studied the density gradient of a system of diffusing particles. The diffusive dynamics starts from an initial configuration of particles which is a fully occupied half lattice adjacent to a completely empty half lattice. A square lattice in the form of an infinite strip of width L parallel to the x axis has been used as the substrate. Initially, each site with x coordinate in the range

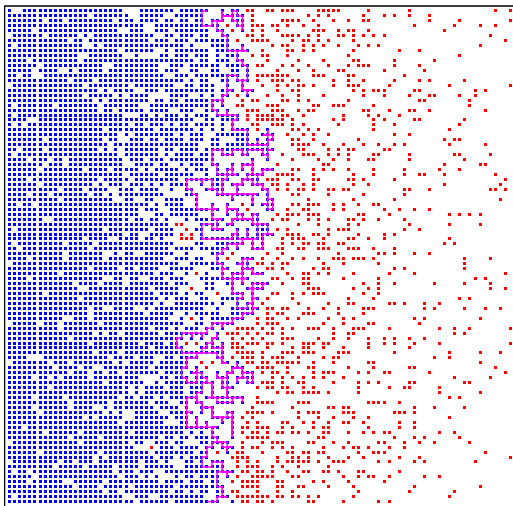


FIG. 8: On an infinite strip of width $L = 100$ placed along the x -axis, particles of an initial density profile with sharp interface starts diffusing. After a time of $T = 128$, the infinite A cluster has been shown by the 3853 blue dots, all finite islands by a total of 1147 red dots and the interface has been marked by the perimeter generating walk of 705 steps shown in magenta color.

$-\infty < x \leq 0$ is occupied by a single particle and rest of the sites have been kept vacant. The average density $\rho(x, T)$ of particles along the vertical line at x is a function of both the position x and the time T . Therefore, as per construction, initially at time $T = 0$, the density profile is a step function at $x = 0$, i.e., $\rho(x, 0) = 1$ for $-\infty < x \leq 0$ and 0 for $x > 0$.

The diffusion dynamics takes place in terms of an infinite sequence of particle hops. In a typical hop a particle selects randomly one of its neighboring sites with uniform probability. The particle moves to that site if and only if the neighboring site is vacant leaving its original site vacant. Clearly, the subset of particles which can at all make successful hops are those which have at least one vacant neighbor. These particles are referred as the ‘active particles’ and their occupied lattice sites are called the ‘active sites’. A lattice bond which has one occupied and one vacant site at its two ends must be located on the perimeter of an island or a lake. Since the diffusion dynamics is limited to these perimeter bonds only, we refer them as the ‘active bonds’. Therefore, an elementary move consists of transferring a particle from one end of the active bond to the other end and is equivalent to interchanging occupied and vacant status of the two end sites of the active bond. The diffusion dynamics constitutes the never ending sequence of such elementary moves.

We have defined that one unit of time T is completed when each active bond is updated once on the average by the random sequential updating procedure.

The algorithm used to study this dynamics has been

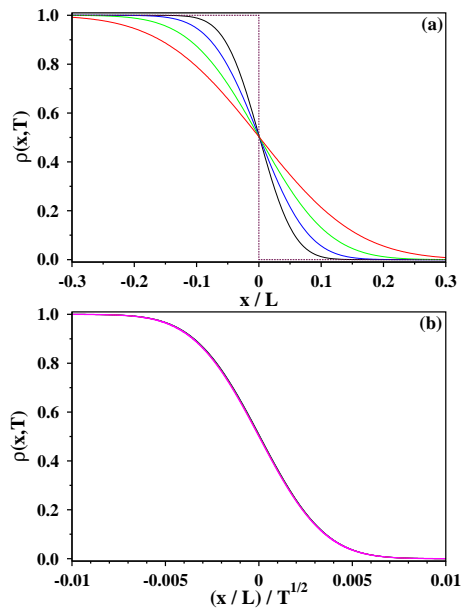


FIG. 9: (a) Average particle density $\rho(x, T)$ has been plotted against the scaled coordinate x/L for the system size $L = 512$ at different instants of time, e.g., $T = 0$ (dashed line), 256 (black), 512 (blue), 1024 (green), and 2048 (red). (b) The same data have been replotted after a further scaling of the x -axis by a factor $T^{1/2}$. In addition, we have plotted half of the complimentary error function $(1/2)erfc(x/256)$ (magenta) to obtain an excellent collapse of the four scaled data sets and the function.

described in the following. At any intermediate stage, the list of all active bonds are stored in an array, called ‘List’. For every active bond i in the List its corresponding lattice bond is assigned the number i . These numbers are stored in the array ‘Bondnumber’.

An elementary move of the diffusive dynamics consists of selecting one of these active bonds ‘ i ’ randomly, with uniform probability. On the square lattice, the end sites of i are the meeting points of six other neighboring bonds, and in general some of them are active and rest are inactive. The occupied and vacant status of the end sites of the bond i are now interchanged. As a result, the status of the bond i remains unchanged but the active / inactive status of the six neighboring bonds of i are reversed. The neighboring bonds which were active prior to the elementary move are now inactive and they are removed from the List array and its length is shortened accordingly. The numbers associated with the corresponding bonds in the Bondnumber array are made zero. On the other hand, the bonds which were inactive before the elementary move have now become active and therefore they are included in the List array, its length is increased, and their bond numbers are stored in the Bondnumber array.

A snapshot of the particle configuration on an infinite strip placed along the x -axis and of width $L = 100$ has been shown in Fig. 8. Particles have been marked by the blue dots. At time $T = 128$ many islands of occu-

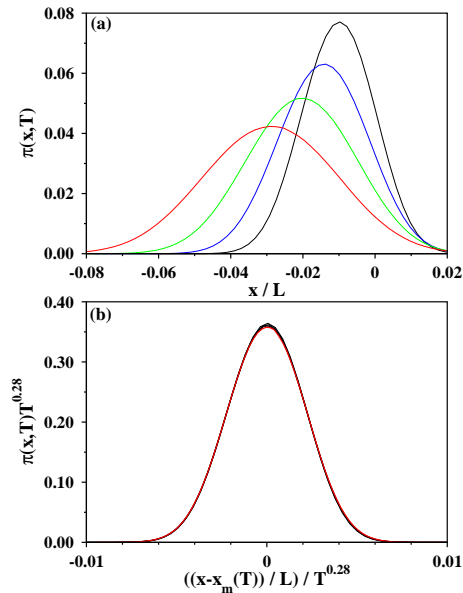


FIG. 10: (a) The interface of the infinite A cluster of diffusing particles flattens with time. The density $\pi(x, T)$ of the occupied sites on the interface has been plotted against the scaled coordinate x/L at different time instants of time, e.g., $T = 256$ (black), 512 (blue), 1024 (green), and 2048 (red). Each curve fits excellent to a Gaussian and the location $x_m(T)$ of the maximum has been obtained from the fit. As time passes the location of the maximum drifts to the left, i.e., towards the high density region. (b) The same data has been replotted, first by shifting an amount $x_m(T)$ and then scaling both the axes by the same time dependent factor $T^{0.28}$ which exhibits nice collapse of the data.

pied sites are visible within the initially vacant half strip. Similarly, many lakes of vacant sites are visible within the initially occupied half strip. Using the algorithm of ‘perimeter generating walk’ [10] the external hull of the infinite ‘A’ cluster has been marked.

The density $\rho(x, T)$ of particles has been estimated as a function of x and at different instants of time T . The density has been averaged over all sites on the vertical line from $y = 1$ to L and therefore it is not dependent on the y coordinates. In Fig. 9(a) we have plotted the density $\rho(x, T)$ for the strip width $L = 512$ against x/L for the five different values of T , namely, $T = 0, 200, 400, 800,$ and 1600 . After the initial step function, the density profile systematically flattens as the time proceeds. In Fig. 9(b) we have replotted the same data but scaled the x/L axis by $T^{1/2}$ to obtain the best collapse of the data. Further, in the same figure we have plotted half of the complimentary error function $(1/2)\text{erfc}(x/256)$ using the magenta color to obtain an excellent data collapse.

As the density profile flattens with time, so also the interface of the infinite A cluster. Like gradient percolation we have defined the interface of the infinite A cluster as the set of occupied sites which have at least one vacant

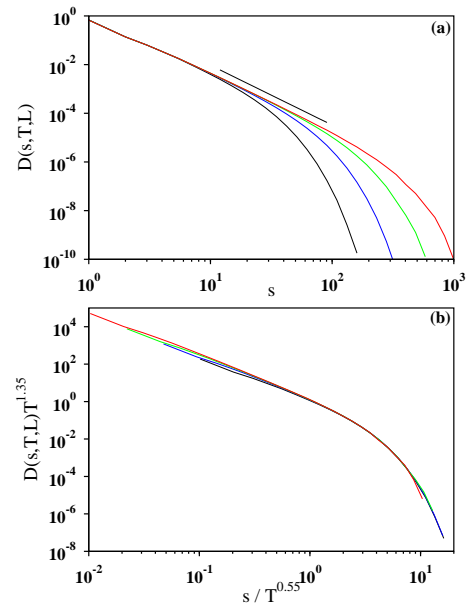


FIG. 11: (a) The probability distribution $D(s, T, L)$ of island sizes at time T has been plotted against the island size s of diffusing particles on an infinite strip of width $L = 1024$. Four sets of data have been shown e.g., for $T = 64$ (black), 256 (blue), 1024 (green), 4096 (red). A direct estimation of the slope of the curve for $T = 4096$ at its longest linear region yields an average value $\tau \approx 2.45$, indicated by the shifted straight line. (b) The same data have been replotted after scaling the axes using the time dependent factors $T^{0.55}$ and $T^{1.35}$ for the x and y axes respectively. This analysis also gives the same value of $\tau = 1.35/0.55 \approx 2.45$.

site in the neighboring, or next neighboring sites that is connected via at least one path of B atoms to $x = +\infty$. At an arbitrary intermediate time, we have marked the occupied sites on the interface using the perimeter generating walk [10]. The density of these interface sites is denoted by $\pi(x, T)$. Initially, it is a delta function at $x = 0$. As time proceeds the density profile of the interface gradually expands in width and at the same time its height becomes shorter. However, the density profile fits to the Gaussian very well at all times and its peak position drifts slowly along the negative x -axis. In Fig. 10(a) we have plotted the interface density profile for four different values of T , namely, for $T = 256, 512, 1024$ and 2048 . For each curve, we have denoted the peak position by $x_m(T)$ and find that it shifts with time as: $x_m(T) \propto T^{0.509}$. In Fig. 10(b) we have first shifted the x -axis by an amount equal to $x_m(T)$ so that the peak positions are on the same vertical line. Then we have tried to scale the x and y axes using a tunable power of time T for a possible data collapse. It is found that a plot of $\pi(x, T)T^{0.28}$ against $(x - x_m(T))/T^{0.28}$ gives the excellent data collapse of all four curves.

Finally, the island size distribution $D(s, T, L)$ has been estimated for different values of time T and system width L . In Fig. 11(a) we have plotted the distribution

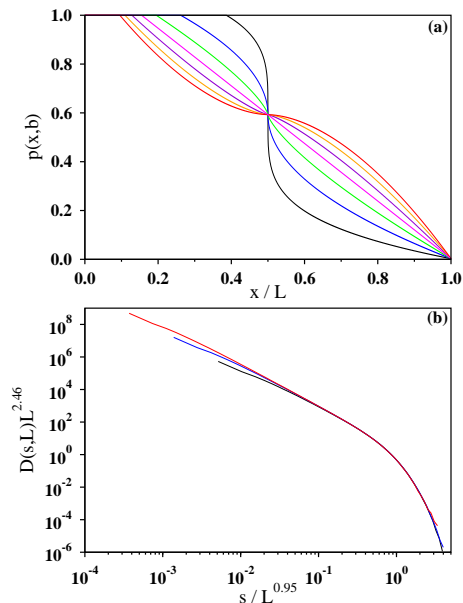


FIG. 12: (a) Nonlinear occupation probability $p(x,b)$ has been plotted against the scaled x/L coordinate for the values of the power $b = 0.25$ (black), 0.50 (blue), 0.75 (green), 1.00 (magenta), 1.25 (maroon), 1.50 (orange), and 1.75 (red). A value of $L = 4096$ has been used for this plot. (b) Finite size scaling analysis for the island size probability distribution using the nonlinear percolation occupation probability with power $b = 0.75$ for $L = 256$ (black), 1024 (blue), and 4096 (red).

$D(s, T, L)$ against island size s at four different time instants, namely, $T = 64, 256, 1024$ and, 4096 for $L = 1024$. These four curves are observed to nearly coincide up to the island size ~ 10 , but they separate out from one another for larger sizes. A scaled version of these curves have been plotted in Fig. 11(b). In this figure, the x and y axes have been scaled by the factors $T^{0.55}$ and $T^{1.35}$ respectively. Collapse of the data appear to be quite good. This implies that the value of the power law exponent associated with this distribution is $\tau = 1.35/0.55 \approx 2.45$.

V. NONLINEAR GRADIENT PERCOLATION

Finally, following the work of Gastner and Oborny [15], we have studied the probability distribution of the island sizes in a gradient percolation problem where the percolation occupation probability $p(x)$ is a nonlinear function of x . More precisely, if the value of the percolation threshold p_c occurs at x_c then in this case the percolation probability varies with the x coordinate as $|p(x) - p_c| = a|x|^b$ where a and b are the tunable parameters.

In our simulation algorithm on the $L \times L$ square lattice we have assumed that $p = p_c$ occurs at $x = L/2$. The value of a has been kept fixed at 0.59 where as seven different values of the parameter b have been studied (Fig.

b	$\alpha(b)$	$\beta(b)$	$\tau(b)$
1.75	1.321	3.01	2.28
1.50	1.268	2.948	2.325
1.25	1.19	2.84	2.39
1.00	1.08	2.645	2.45
0.75	0.95	2.46	2.59
0.50	0.75	2.12	2.83
0.25	0.50	1.90	3.80

TABLE I: Values of the island size distribution exponent $\tau(b)$ as well as the scaling exponents $\alpha(b)$ and $\beta(b)$ for different values of b in the nonlinear gradient percolation model.

12). A large number of independent percolation configurations have been generated with this prescription and the statistics of island sizes have been collected as before. Using the Eqn. (1) again, a similar scaling analysis has been performed and the scaling exponents $\alpha(b)$, $\beta(b)$, and $\tau(b)$ have been found for every value of b . These values have been tabulated in the Table 1.

In Fig. 13 we have shown the plots of $\alpha(b)$, $\beta(b)$ and $\tau(b)$ against b whose values have been listed in table 1. We try to fit their variations using some functional forms. However, without any theoretical argument we try with different functional forms similar to the Eqn. (3) in the paper [15]. We find that indeed a similar functional form exists and the $\alpha(b)$ vs. b data have been fitted nicely by the equation:

$$\alpha(b) = b/(A_1 b + A_2). \quad (2)$$

where $A_1 = 0.528$, $A_2 = 0.395$. It may be noted that the ratio $A_1/A_2 \approx 1.337$ which is very close to the correlation length exponent $\nu = 4/3$ of the ordinary two dimensional percolation. On the other hand, the values of $\beta(b)$ vs. b and $\tau(b)$ vs. b have been fitted by the equations:

$$\begin{aligned} \beta(b) &= \sqrt{b}/(B_1 \sqrt{b} + B_2) & \text{and} \\ \tau(b) &= \sqrt{b}/(T_1 \sqrt{b} + T_2). \end{aligned} \quad (3)$$

where $B_1 = 0.177$, $B_2 = 0.200$ and $T_1 = 0.539$, $T_2 = -0.132$.

We thank the anonymous reviewer who pointed out that a negative value of T_2 would imply $\tau(b)$ to be infinite when $b \approx 0.06$. We believe that such a small non-zero value of b is due to the numerical uncertainties. Truly, the value of τ should be infinite for $b = 0$, since for this value the probability function $p(x)$ is discontinuous as a step function. The islands occur only in the $x > L/2$ region where the value of $p(x) < p_c$ and therefore all islands in the sub-critical region are the small size clusters. Like the ordinary percolation the probability distribution of these clusters should have an exponential tail which is effectively equivalent to a power law tail with $\tau = \infty$.

VI. SUMMARY

To summarize, we have revisited the well known problem of gradient percolation. In this problem, the sites of

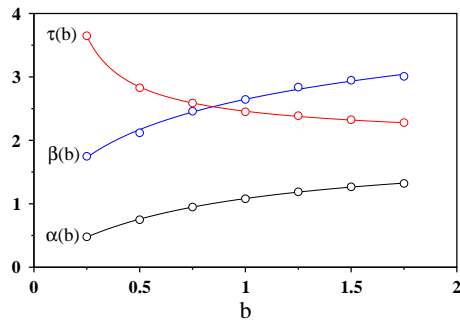


FIG. 13: The best estimates of the finite size scaling exponents $\alpha(b)$ and $\beta(b)$ and the island size distribution exponent $\tau(b)$ have been plotted against the nonlinear power b for seven different values of b . The data for $\alpha(b)$ vs. b (black) have been best fitted by Eqn. 2 where as $\beta(b)$ vs. b (blue) and $\tau(b)$ vs. b (red) have been best fitted by Eqn. 3. The data points have been shown by the circles where as the fitted curves have been shown by the continuous lines.

a regular lattice are occupied with a probability $p(x)$ that is a function of the x coordinate of the site. In the sections II and III, this function has a linear gradient with a constant negative slope g along the x -axis where we have done the calculation using the two methods, namely (i) the gradient site percolation, and (ii) the gradient bond percolation. The model has been simulated on a square lattice of rectangular shape whose width L_x may be a

maximum of $1/g$ and the height L_y . The islands are the clusters of occupied sites within the infinite vacant cluster and the lakes are the clusters of vacant sites within the infinite occupied cluster. The probability distribution of the island sizes have been studied and found to follow a power law distribution with an exponent τ . For $L_x \sim 1/g$ the value of $\tau \approx 2.45$ is obtained which is distinctly different from the value of the same exponent of the ordinary two dimensional percolation problem. However, when $L_x \ll 1/g$ one retrieves back the percolation cluster size exponent $\tau = 2 + 5/91 \approx 2.05$. Further in section IV, we have studied the same distribution for a system of randomly diffusing particles starting from a dense region. To the best of the accuracy of our simulations and analysis of the statistical data, we find very strong indications that the value of the exponent $\tau \approx 2.45 \pm 0.02$ is indeed different from $5/2$ though we cannot strictly rule out the small possibility that they may be the same. Finally, in section V we have studied the island size distribution again for the nonlinear gradient percolation following the work of Gastner and Oborny [15]. We have observed that the island size distribution exponent τ is indeed an explicit function of the nonlinear parameter b .

It's my great pleasure to congratulate Professor R. M. Ziff (Bob) on his 70th birth year. I wish him a truly fabulous birth year and many more productive and successful years to come. I also thankfully acknowledge Bob for many helpful discussions on this work and for the critical reading of the manuscript.

-
- [1] B. Sapoval, M. Rosso, and J. F. Gouyet, *J. Physique. Lett.* **46**, L149 (1985).
 - [2] M. Rosso, J. F. Gouyet, and B. Sapoval, *Phys. Rev. B.* **32**, 6053 (1985).
 - [3] M. Rosso, J. F. Gouyet, and B. Sapoval, *Phys. Rev. Lett.* **57**, 3195 (1986).
 - [4] S. Broadbent and J. Hammersley, *Percolation processes I. Crystals and mazes*, Proceedings of the Cambridge Philosophical Society **53**, 629 (1957).
 - [5] D. Stauffer and A. Aharony, *Introduction to Percolation Theory*, Taylor & Francis, (2003).
 - [6] G. Grimmett, *Percolation*, Springer (1999).
 - [7] M. Sahimi. *Applications of Percolation Theory*, Taylor & Francis, 1994.
 - [8] W. Dietrich, P. Fulde and I. Peschel, *Adv. Phys.* **29**, 527 (1980).
 - [9] R. F. Voss, *J. Phys. A* **17**, L373 (1984).
 - [10] R. M. Ziff, P. T. Cummings, and G. Stell, *J. Phys. A: Math. Gen.* **17**, 3009 (1984).
 - [11] R. M. Ziff, *Phys. Rev. Lett.* **56**, 545 (1986).
 - [12] R. M. Ziff and B. Sapoval, *J. Phys. A: Math. Gen.* **19**, L1169 (1986).
 - [13] J. Tencer and K. M. Forsberg, *Phys. Rev. E* **103**, 012115 (2021).
 - [14] J. L. Jacobsen, *J. Phys. A: Math. Gen.* **48**, 454003 (2015).
 - [15] M. T. Gastner and B. Oborny, *New J. Phys.* **14**, 103019 (2012).